

5-2016

Isolation of Metallic Single-Walled Carbon Nanotubes for Electrically Conductive Tissue Engineering Scaffolds

Jakob Hockman
University of Arkansas

Follow this and additional works at: <http://scholarworks.uark.edu/bmeguht>

 Part of the [Biomaterials Commons](#), and the [Molecular, Cellular, and Tissue Engineering Commons](#)

Recommended Citation

Hockman, Jakob, "Isolation of Metallic Single-Walled Carbon Nanotubes for Electrically Conductive Tissue Engineering Scaffolds" (2016). *Biomedical Engineering Undergraduate Honors Theses*. 39.
<http://scholarworks.uark.edu/bmeguht/39>

This Thesis is brought to you for free and open access by the Biomedical Engineering at ScholarWorks@UARK. It has been accepted for inclusion in Biomedical Engineering Undergraduate Honors Theses by an authorized administrator of ScholarWorks@UARK. For more information, please contact scholar@uark.edu, ccmiddle@uark.edu.

Isolation of Metallic Single-Walled Carbon Nanotubes for Electrically Conductive Tissue Engineering Scaffolds

By: Jakob T. Hockman
Department of Biomedical Engineering

Faculty Mentor: Dr. Jin-Woo Kim
Department of Biological Engineering

Abstract

Metallic single-walled carbon nanotubes (m-SWNTs) were separated from pristine SWNTs using affinity chromatography for use in electrically conductive tissue engineering scaffolds. Approximately one third of SWNTs have metallic properties. Separations were achieved using a protocol modified from Liu & coworkers (2011) in order to improve the method for cell culture environments. Samples enriched in m-SWNTs were isolated and characterized. However, challenges still remain for the complete separation of m-SWNTs from their semiconducting counterpart (s-SWNTs) using this protocol. Approaches to improve separation and reduce the difficulties associated with processing the nanotubes were suggested. One of the ultimate destinations of these nanotubes would be conductive m-SWNT and collagen hydrogels for neuromuscular tissue engineering scaffolds.

Background and Significance

Tissue Engineering Scaffolds

Tissue engineering (TE) scaffolds control the growth and development of cells by mimicking the environment in which they normally grow and function. In the human body, most cell types grow and function anchored to an extra-cellular matrix (ECM). Thus, in many cases designing a tissue engineering scaffold is an attempt to replicate the ECM of a particular cell type.

Electrically conductive scaffolds are used to simulate the electrically active environment in which cells in neuromuscular tissues normally grow. Electrical stimulation (ES) mimics natural ion movement through the cell membranes (Figure 1) and causes downstream effects normally associated with action potentials (Gheith et al., 2006). These effects are linked to the proliferation and differentiation of neuromuscular cell cultures (Ghasemi-Mobarakeh et al., 2009). Liu & coworkers (2009) have shown the effects of ES is dependent on the electrical properties of the scaffold. They were able to enhance the amount of differentiation by changing the ratio of conducting to non-conducting fibers in the copolymer scaffold. Thus, the effects of ES can be enhanced by improving the electrical properties of the scaffold. The major difficulties with synthetic materials in TE scaffolds are lack of biocompatibility and bioactivity.

Modified single-walled carbon nanotubes (SWNTs) are both conductive and biocompatible and have shown much promise in neuromuscular TE. SWNTs have been used to enhance cultures of PC-12 neuronal cells (Gheith et al., 2006), aortic smooth muscle cells

(MacDonald et al., 2005), and C2C12 myocytes (Ahadian et al., 2014). Most applications have used pristine nanotubes, which are mixtures of semiconducting SWNTs (s-SWNTs) and metallic SWNTs (m-SWNTs). However, m-SWNTs are more conductive than their semiconducting counterparts. Thus, isolating m-SWNTs from mixtures of pristine nanotubes would improve the electrical properties of the nanotubes and could then be used to enhance the effects of electrically stimulating neuromuscular cell cultures.

Separation of SWNTs

Conceptually, SWNTs are cylinders composed of interconnected carbon rings. Their properties are determined the chiral wrapping vector, or (n,m) vector, which defines how the carbon rings are connected to each other (Figure 2). For some geometries, the twist in the chains of carbon atoms causes strain to the carbon-carbon

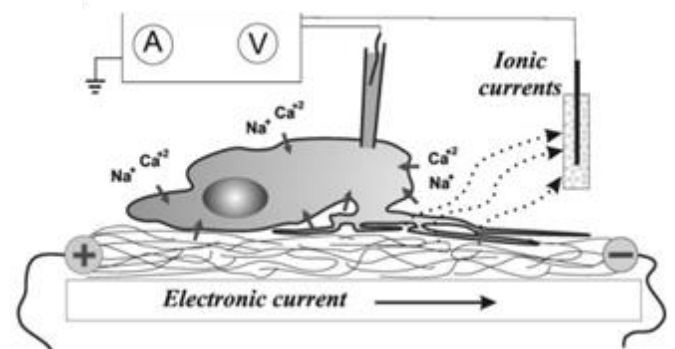


Figure 1: Electrical stimulation of neuromuscular cells (Gheith et al., 2006). Current through conductive TE scaffolds opens ion channels in the cell membrane and mimics action potentials, causing changes in protein expression and cell differentiation.

bonds which increases the energy of the electrons (Niyogi et al., 2002). If the electrons are high enough in energy, they can conduct electricity. This occurs at very specific geometries when the difference between the chiral wrapping indices are divisible by three ($(n-m)/3$) (Saito et al., 1998). If $n-m$ is not divisible by three, the nanotube is semiconducting and can conduct electricity only when energy has been added to the system, e.g. an increase in temperature, absorbance of light, etc. Therefore, approximately one third of all SWNTs take on metallic properties and two thirds take on semiconducting properties according to theoretical predictions and experimental evidence (Wilder et al., 1998).

SWNTs are quasi 1-dimensional quantum wires because the electrons in the outer shell move favorably along the longitudinal axis instead of the circumferential axis (Barone et al., 2012). Because of this, there are constraints on the energy levels that an electron can occupy. The number of available states for an electron to occupy at a particular energy level is called the density of states, or DOS function. Single-walled carbon nanotubes and other quasi 1-dimensional materials contain a large number of states at the energy levels allowed by the directional constraints and a low number at those forbidden. Because of this, SWNTS show sharp peaks in the DOS function at those energy levels allowed by the directional constraints (Figure 3a). These peaks are called Van Hove singularities and they are separated from each other by regions of low or zero-level gaps termed energy gaps. These gaps are known as band gaps in semiconducting tubes since there is a zero-level DOS in between the first Van-Hove peaks. This gap represents the amount of energy that needs to be added to the system in order for the tubes to conduct electricity. The gaps in the metallic nanotubes are in general larger than the ones in the semiconducting nanotubes, though in metallic nanotubes they are not true band gaps since there is a finite density of states between them and electrons can freely conduct electricity at all energy levels. The energy gaps in metallic nanotubes represent the difference between two energy levels at which conductivity experiences a sharp increase, i.e. energy levels at which conduction occurs favorably (Wilder et al., 1998).

Optical transitions occur when an incident photon carries an energy equal to one of the energy gaps between Van-Hove singularities. A photon that has the specific amount of energy necessary to make a nanotube jump from one peak in the DOS to the corresponding level on the other side of the gap will be strongly absorbed by the material. These peak absorbances are shown by the presence of Van-Hove peaks throughout the visible and

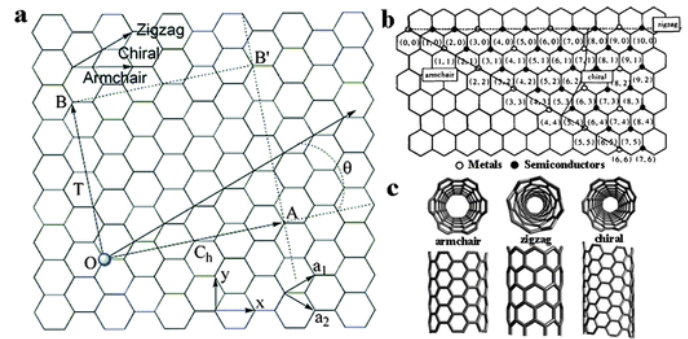


Figure 2: Chiral Wrapping Vector (Zhang et al., 2011). A. Wrapping vector determines zigzag, armchair, or chiral nature of nanotubes. B. Wrapping vector determines electronic (metallic or semiconducting) properties. C. Wrapping vector determines geometry and energy level of electrons in nanotube.

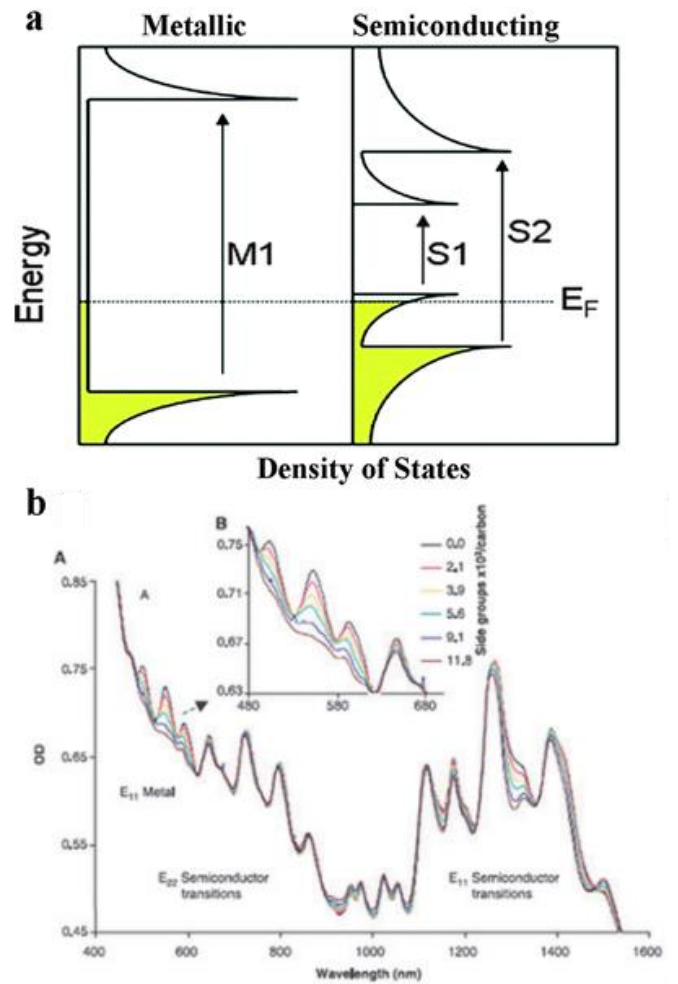


Figure 3: Density of states and optical transitions of SWNTs (modified from Zhang et al., 2011). A. Energy gaps in metallic and semiconducting SWNTs. Metallic gaps are larger, requiring more energy to transition. E_f = fermi energy. B. SWNT absorbance spectra. Metallic peaks in higher energy/lower wavelength region, semiconducting in higher wavelength.

near-infrared wavelengths in an absorbance spectra (Figure 3b). Because of the differences in energy gaps, metallic nanotubes absorb higher energy, lower

wavelength light and semiconducting nanotubes absorb lower energy, higher wavelength light.

When nanotubes are individually dispersed, they show these Van Hove throughout their absorbance spectra because of the constraints to electron motion (Figure 3b). However, when nanotubes are present in bulk phase or are clumped together in solution, electron can flow just as easily across the surface of neighboring nanotubes as they can down the longitudinal access so they do not experience the directional constraint and will show an absorbance spectra free of Van Hove peaks. This property can be used to determine the concentration of nanotubes in solution that are individually dispersed.

SWNTs can be individually dispersed using a sonicator and a surfactant, though this process is dependent on the strengths of both the sonicator and surfactant. Three commonly used surfactants are sodium dodecylbenzenesulfonate (NaDBS), Triton X-100, and Sodium Dodecyl Sulfate (SDS) (Figure 4). NaDBS and Triton X-100 are both strong surfactants because of pi-stacking interactions between their aromatic rings and the SWNT sidewalls (Kotagiri & Kim, 2014). SDS is a much weaker surfactant but has special properties that can be used to separate nanotubes based on electronic subtype.

SDS is an amphiphilic molecule with a long, hydrophobic tail and anionic sulfate head (Clar et al., 2013). The dispersion of SWNTs in SDS relies on strong sonication to form SDS micelles around the nanotubes. The hydrophobic tails aggregate on the sidewalls of the nanotubes while the anionic head creates mirror charges in the carbon atoms.

The primary difference between m-SWNTs and s-SWNTs is the strength at which electrons are bound to the carbon atoms. The electrons in m-SWNTs are at higher energies and weakly bound which increases their mobility and facilitates conduction of electricity. Additionally, m-SWNTs are more easily polarized than s-SWNTs as the electrons in the outer shell can easily shift away from the negatively charged sulfate head in SDS to the other side of the carbon atoms, or “mirror” its charge. As a result, m-SWNTs form stronger dipoles with SDS which strengthens binding. (Clar et al., 2013) In general m-SWNTs have a more consistent coat of SDS molecules than do s-SWNTs. This property can be used to separate SWNTs based on electron subtype.

Affinity chromatography can be used to separate SDS dispersed nanotubes (Clar et al., 2013). SDS interferes with the ion-dipole interactions between the nanotubes and gel media that normally cause nanotubes to bind to the gel (Figure 5). The m-SWNTs are passed through the gel because of their SDS coating while s-SWNTs are retained. The s-SWNTs can be eluted

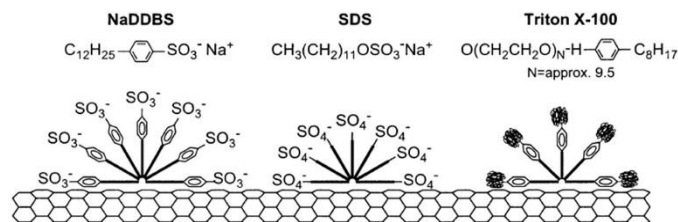


Figure 4: Commonly used surfactants for single-walled carbon nanotube dispersion (Xin et al., 2013). Aromatic rings present in NaDDBS (NaDBS) and Triton X-100.

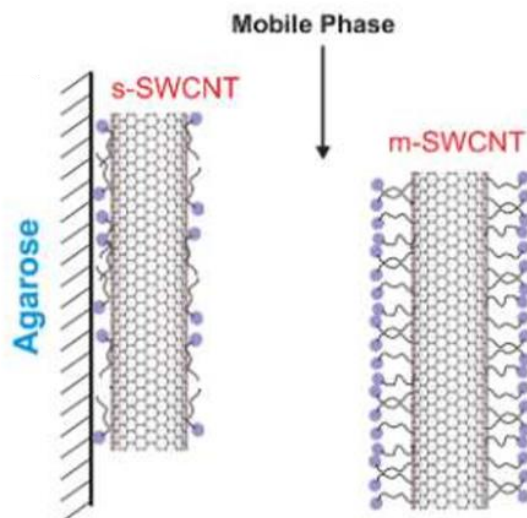


Figure 5: Favorable coverage metallic nanotubes (Clar et al., 2013). m-SWNTs freely pass with mobile phase (2% SDS) while s-SWNTs are retained in gel.

afterwards with a higher concentration SDS solution or a stronger surfactant, e.g. 2% sodium deoxycholate (DOC). Liu & Coworkers (2011) were able to separate SWNTs by electronic subtype using affinity chromatography with Sephacryl S-200 gel. However, their nanotube samples were dispersed using a tip-sonicator for 24 hours. This type and length of sonication exposed the rest of the lab to SWNT contamination because of the open sample container. The use of a cup-sonicator to disperse nanotubes would be much less efficient but much safer for cell-culture environments. Thus, the specific aims of these experiments were to: (1) separate SWNTs that had been dispersed with a cup sonicator and (2) overcome inherent limitations of using a less powerful sonicator.

Materials and Methods:

Preparation of SWNTs

SWNT sample preparation was modified from previously reported protocols (Kim et al., 2006). 2.5 mg of SWNTs (Unidym, Lot No: R1794) and 40 mg of SDS (Sigma Aldrich, Lot: 043K0014) were added to 5ml of ddH₂O for a .5 mg/ml concentration of SWNTs in 2%

SDS solution. The vial was secured in a cup sonicator (Virsonic 600 Ultrasonic Homogenizer) and subjected to cyclic sonication at 65% maximum power for 1-1.5 hours total process time (10 minutes on, 10 minutes off for 2-3 hours respectively). The solution was centrifuged in a micro centrifuge (Beckman Coulter Microfuge 18) at maximum power (18,000 x g) for 30 minutes to remove aggregates. The upper 80-85% of supernatant was collected and placed in a new vial for the separation experiments. UV-Vis spectroscopy (Beckman Coulter DU-800 Spectrophotometer) was performed both pre- and post-centrifugation to determine the dispersion efficiency.

Preparation of Gel Columns

The columns (syringes) were prepared by plugging the top of a 20 gauge needle with cotton and attaching it to the bottom of a syringe (3 or 10ml). 2 ml of Sephacryl S-200/20% ethanol solution (GE Healthcare, Lot: 10223200) was added to one of the columns followed by .5 ml of 2% SDS solution. The gel beads settled to ~1.4ml in volume and aliquots of 2% SDS were added until a total of 5ml of 2% SDS had been passed through to wash away any ethanol.

Separation of SWNTs

Separation was carried out as previously described by Liu & coworkers (2011). 1ml of the pristine nanotubes (or 3ml of 3x diluted nanotubes) was added to a gel column. Collection was started once the nanotubes had visibly reached the bottom of the gel. 2% SDS solution was added (~ 4ml) until the eluted solution became transparent. 5% SDS was then added to column until the flow also became transparent (~ 4ml). Finally, 2% sodium deoxycholate (~ 4ml) until no other nanotubes could be eluted from the gel. Samples were measured using UV-Vis spectroscopy and compared to published data from Liu & coworkers (2011). Electron microscopy images of the nanotubes were procured using a Jeol TEM and were analyzed in ImageJ.

Results and Discussion

Analytical Method for Characterizing SWNTs

Selected data from Liu & coworkers (2011) were used as a reference for each separation experiment. The absorbance spectra of their samples (Figure 6) showed characteristic peaks in the lower wavelength range from 450nm – 650nm as well as a drop in absorbance in the 800-1000nm range for the metallic sample, which was

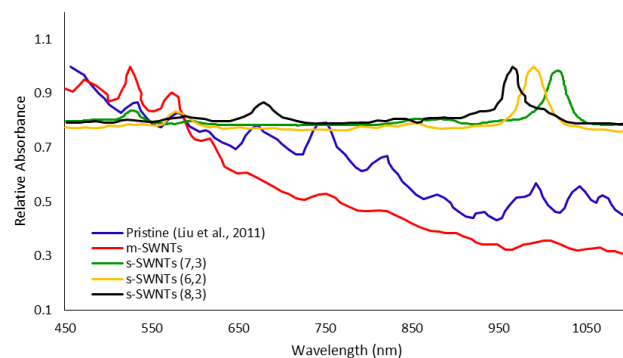


Figure 6: Selected data from Liu & coworkers (2011). Clear enrichment in lower wavelength region for metallic samples and higher wavelength peaks for semiconducting samples. Semiconducting samples had peaks at ~ 1030, 980, and 960nm.

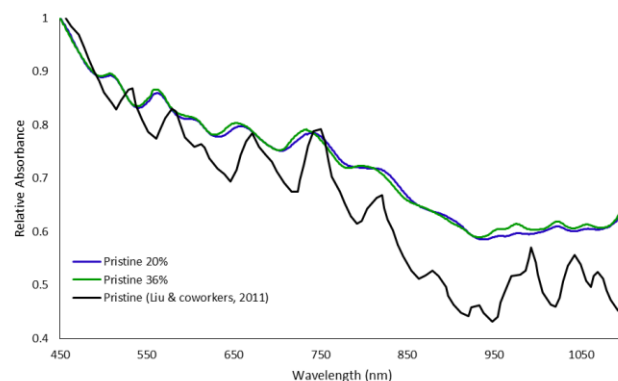


Figure 7: Comparison of starting SWNT samples. Van Hove peaks are much more pronounced in sample by Liu & coworkers (2011), suggesting their nanotubes were more individually dispersed than the samples used here.

consistent with the theory behind SWNT optical transitions. The semiconducting samples showed characteristic peaks at 960, 980, and 1030nm depending on the (n,m) chirality of the nanotubes. The semiconducting samples also showed a drop in absorbance in the 450-650nm range, which was also consistent with predictions. These results show that separation of metallic from semiconducting SWNTs could be confirmed with absorbance measurements. This analytical method was used to determine the success of the following separation experiments. The samples eluted with 2% SDS were referred to as m-SWNTs. The samples eluted with 5% SDS or 2% DOC were named s-SWNT sample to remain consistent.

Dispersion Efficiencies

Absorbance measurements pre- and post-centrifugation were used to determine the dispersion efficiency of 1 and 1.5 hours sonication times (Figure 7). The ratio of SWNT concentrations before and after centrifugation provides a rough estimate of the

concentration of SWNTs that were individually dispersed or present in small bundles. On average, 1 hour of sonication dispersed 20% of the nanotubes and 1.5 hours dispersed 37%.

The Van Hove peaks in the pristine nanotube sample were much more pronounced in the work by Liu & coworkers, suggesting that their SWNTs were on average more individually dispersed. They also had much greater absorbance in the NIR region, which suggested that their sample was enriched in s-SWNTs. This would confirm the order of SDS binding to the nanotubes. SDS binds preferentially to m-SWNTs so it required more sonication to disperse s-SWNTs. Compared to the 20% dispersed sample, 37% dispersed nanotubes also had larger peaks in the 900-1100nm range, which confirmed that higher sonication efficiencies enrich samples in s-SWNTs. The differences in absorbance spectra between starting materials made it difficult to compare numerical data between experiments. However, the peak absorbances in each nanotube samples were compared against the published data to confirm the enrichment of either metallic or semiconducting SWNTs.

Separation with 20% Dispersed Nanotubes

Separation was performed on the 20% dispersed nanotube sample and these results are shown in Figure 8. The later eluted s-SWNT samples showed characteristic peaks at ~1000 nm and ~960 nm. These results were consistent with the changes in peak absorbance as the separation order increased as described by Liu & coworkers, 2011). This suggested that s-SWNT samples were successfully being separated by chirality.

However, the m-SWNT sample showed an overall lower absorbance in all regions of the spectrum and had a characteristic peak at ~1040nm which was not consistent with the data from Liu & coworkers (2011). In fact, the 1040nm peak in this sample was similar to the 1020nm peak of the first s-SWNT sample from Liu & coworkers (2011). This could only happen if m-and s-SWNTs were eluted at the same time. Additionally, there seemed to be metallic enrichment in the first s-SWNT sample eluted by 5% SDS as visible by the increase in absorbance in the 450-650 nm range. This suggested that the interactions between the gel and the nanotubes were dependent on factors other than SDS binding or that SDS binding was not occurring according to predictions.

It was hypothesized that the nanotubes were dispersed in small bundles of metallic and semiconducting SWNTs. These bundles would show

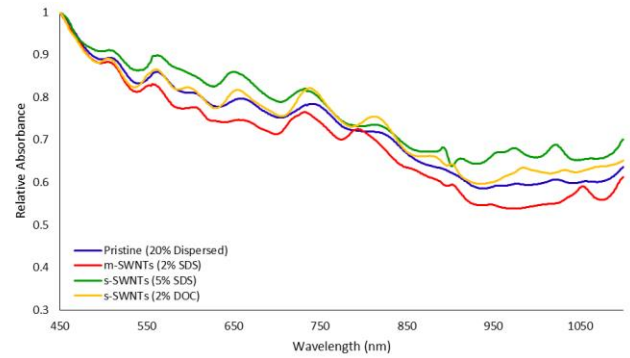


Figure 8: Separation with 20% dispersed SWNTs. Clear peaks in s-SWNT samples in 900-1000 nm range. 2% SDS Sample has 1050 nm peak, characteristic of m-SWNTs. 5% SDS sample has peak at ~1010nm. 2% DOC has peak at ~ 970 nm.

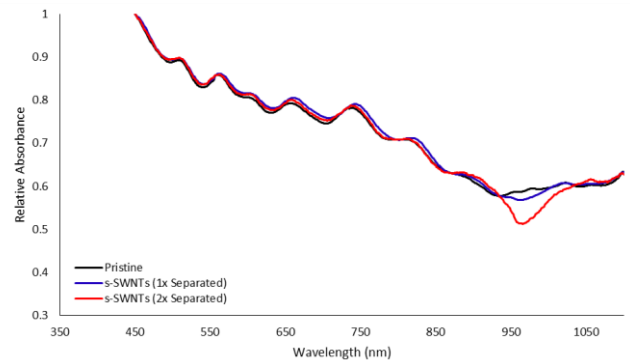


Figure 9: Characteristic peak at ~1040 nm in second separated sample was not present in first separated sample. Suggests that s-SWNTs with 1040nm peak pass through gel quicker than other s-SWNT samples.

peak wavelengths dependent on the relative concentration of m- or s-SWNTs contained. These bundles would also prevent metallic SWNTs to be distinguished from semiconducting SWNTs during the separation process. Thus, it was likely that the m-SWNT sample contained both metallic nanotubes and those semiconducting nanotubes that bound easiest to SDS molecules. This would account for the 1040 nm peak in the metallic SWNT sample.

In a follow-up experiment, the first eluted s-SWNT sample in 5% SDS was sonicated for an additional fifteen minutes to determine if SDS would cover those s-SWNTs that produced the 1040nm peak. These nanotubes were then separated using the standard method to see show the differences in absorbance spectra before and after separation. Most of the s-SWNTs remained bound to the gel after the second round of separation. However, those nanotubes that were eluted showed the 1040nm peak (Figure 9). This would support the hypothesis that metallic and semiconducting SWNTs were eluted together and that SDS preferentially covered those s-SWNTs with the 1040nm peak.

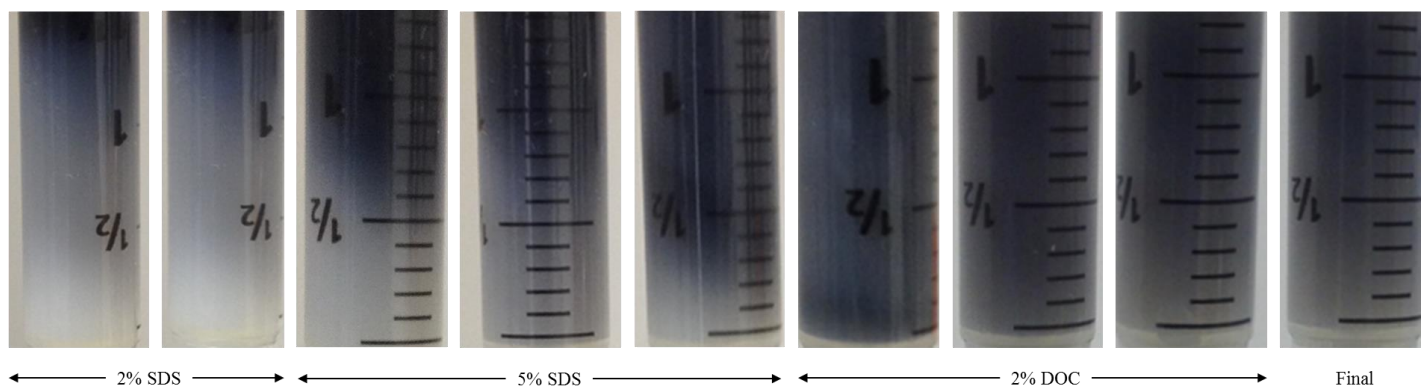


Figure 10: Separation process. Each surfactant reached a maximum amount of SWNTs that it could effectively elute from the gel. Even 2% DOC reached a cutoff point after which no more SWNTs could be eluted from the gel.

These results showed that the process could not distinguish between m- and s-SWNTs. Since this result was not reported by Liu & coworkers (2011), it was likely that there were additional interactions between the nanotubes and gel that had not been accounted for or that SDS binding was not occurring as the theory suggested. In order to test these hypotheses, different interactions between the nanotubes and gel were isolated and tested one-by-one to determine which was responsible for the lack of resolution during separation.

Permanent SWNT/Gel Binding

Figure 10 shows the progression of a typical separation experiment. Each surfactant visibly moved the nanotubes further down the gel until it could no longer elute any SWNTs from the opening. The final image in the progression shows that some nanotubes remained in the gel even after 2% DOC was added. This result suggested that the interactions between the nanotubes and the gel were stronger than those reported by Liu & coworkers (2011) and that this was negatively influencing separation.

The interactions between the nanotubes and gel were divided into two categories: physical and chemical interactions. The physical factors explored were size, concentration, and flow rate of SWNTs in the gel. The chemical factors explored primarily concerned SDS coating of nanotube sidewalls. Each of these factors was individually explored in order to determine which was responsible for the permanent binding of the nanotubes to the gel.

Effect of Nanotube Size

The first hypothesis tested was that the SWNTs were too small such that they entered into the pores of the gel and became irreversibly bound, which would have

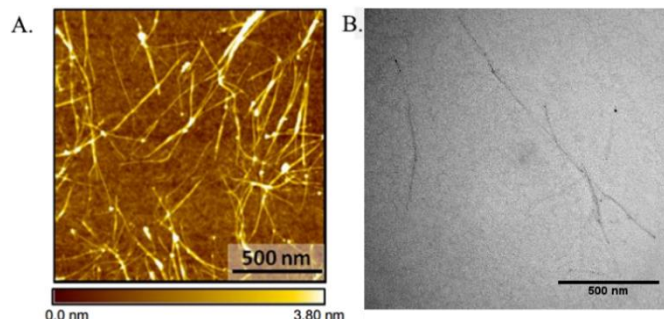


Figure 11: A: AFM image of SWNTs used in separation by Liu and coworkers (2011). B: SEM image of SWNTs used in separation experiments

Table 1: SWNT Length	Liu et al.	Grid 1
Mean SWNT length:	429 nm	430 nm
<i>t-Test Statistic:</i>	0.45	

Table 1: Mean lengths of SWNTs. T-test yielded non-significant difference in nanotube size.

prevented them from being eluted with 2% SDS. To test this, TEM images were taken and compared to the AFM images published by Liu & coworkers (2011). Multiple images were taken but those in Figure 11 are presented as representative images. The mean nanotube length for Liu & coworkers (2011) was 429nm and the nanotubes used here had an average of 430nm. The similarity between these two numbers was impressive though unexpected and the t-test statistic confirmed that the mean nanotube length was not statistically different between the two samples (Table 1). Thus, it is unlikely that the size of individual nanotubes was influencing their interactions with the gel.

Effect of Flow Rate

It was hypothesized that increasing the speed at which the nanotubes flowed through the gel would prevent strong interactions between the gel and SWNTs from accumulating over time. A larger syringe (10ml) and

larger needle (18 gauge) were used to increase the flow rate of the nanotubes. The flow rate was only increased from 1.2 to 1.5 ml/hour using this technique, which was only a 20% increase. This relatively small change in the flow rate was not able to prevent the irreversible binding of the nanotubes to the gel. The extremely long separation time (>8 hours per experiment) was not reported by Liu & coworkers (2011). In fact, their separation experiments took less than 20 minutes to complete, which confirmed that there were differences between the materials and/or methods used to separate. However, based on these results, incremental changes to the flow-rate could not elute any more nanotubes from the gel. It would be possible to increase the flow-rate more dramatically by using a chromatography system. This hypothesis was not tested during these experiments but would be the subject of future projects.

Effect of Nanotube Concentration

In a follow-up experiment, the concentration of the nanotube solution was decreased in an attempt to increase the flow-rate through the gel. It was hypothesized that the sudden introduction of nanotubes to the gel caused a crowding effect and slowed the rate at which the SWNTs passed through the gel. As was described previously, a slow flow rate could have caused the accumulation of nanotube-gel interactions over time. A lower concentration of nanotubes was incrementally added to gel so that the total amount of nanotubes passed through the gel was held constant. In this particular experiment, 3ml of 3x diluted nanotubes were added to the gel (Figure 10C). However, a large proportion of the nanotubes were still permanently bound to the gel, which suggested that nanotube concentration was not the primary reason for irreversible binding.

Potential Removal of SDS from Nanotubes

Based on the previous results, it was determined that physical interactions between the nanotubes and gel were not the primary reason for permanent binding. The next factors tested were chemical interactions.

It was hypothesized that ethanol retained in the gel pores could have influenced how SDS bound to the nanotubes once they entered the gel. Since ethanol is an organic solvent, it was potentially changing the binding coefficient between the nanotubes and gel by favorably interacting with some of the SDS molecules. To test this, a 10ml aliquot of Sephacryl gel was removed from the container and washed vigorously in 2% SDS over the course of 5 hours and left to incubate for an additional 24

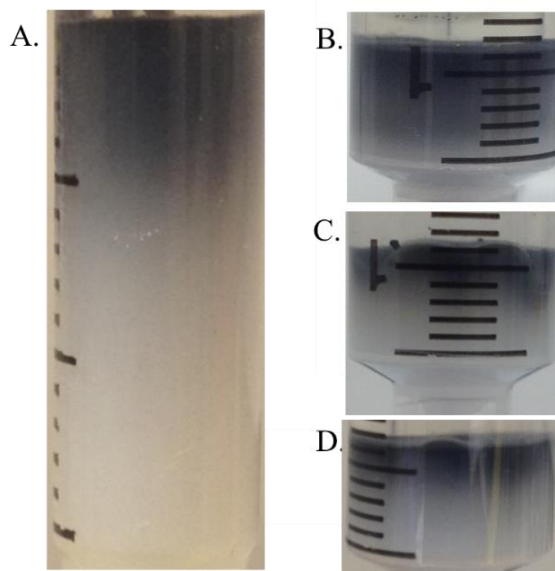


Figure 10 A. Appearance of gel after separation with 20% dispersed nanotubes. B. Larger syringe size. C. Dilution of nanotube sample. D. Gel washing technique. No technique was able to completely elute all of the SWNTs from the gel.

hours before separation was attempted. Visual evidence showed that the SWNTs were still permanently bound to the gel after separation with the washed gel (Figure 10D). This result showed that the ethanol retained in the gel was not responsible for the permanent binding of the nanotubes.

Potential Addition of SDS to Nanotubes

The final hypothesis tested was that the sonication process used to disperse the nanotubes was not allowing for the selective SDS coating of m-SWNTs. The sonication time was increased by 50% in order to test the effects of higher sonication efficiency on the results of separation. The 1 hour-sonicated nanotubes showed a 20% dispersion efficiency whereas the 1.5 hour-sonicated nanotubes showed a 37% dispersion efficiency. This result suggested that SDS binding occurs favorably with longer sonication times since the stability of the nanotubes in aqueous phase is directly caused by SDS coating of the nanotube sidewalls. The 37% dispersed sample also showed enhanced absorption in the s-SWNT band from 900-1100 nm before separation. This suggested that the nanotube sample was already enriched in s-SWNTs before separation.

Because there was almost double the concentration of nanotubes in this sample, the addition of each surfactant had a slightly different effect as compared to the 20% sample. When 2% SDS was passed through the 37% sample, it eluted a much larger amount of SWNTs. The samples eluted with 2% SDS were fractionated based on the time it took to elute and

characterized individually. Interestingly, 5% SDS was unable to elute any nanotubes at all. The extra sonication likely covered the s-SWNTs more fully in SDS molecules which decreased the efficacy of 5% SDS in covering the nanotubes and eluting some from the gel.

The results of the separation process are shown in Figure 11. The m-SWNT sample showed an increase in absorbance in the 450-650 nm band and a decrease in the 800-1100nm band which suggested that this sample was successfully enriched in m-SWNTs. The 1040 nm peak was still present in this sample but was significantly diminished. The second m-SWNT fraction showed a shift in peak wavelength to approximately 1010 nm. This suggested that 2% SDS could be used to elute s-SWNTs provided they are well-dispersed in the sample. The sample eluted with 2% DOC sample showed a peak at ~970 nm, which was consistent with the shifts in peak absorbance as elution order continued.

These results suggested that the separation process could be improved by increasing the sonication efficiency of the samples. However, nanotubes were still bound irreversibly to the gel even after the increased sonication time. It was possible that there were other interactions that were influencing how the nanotubes passed through the gel that influenced both the time and resolution of the separation process. Additionally, the 1040nm peak was still present in the m-SWNT sample, albeit significantly diminished, which suggested that separation could still be improved.

Conclusion

We successfully demonstrated that the method used by Liu & coworkers (2011) could be modified for use in a cell culture environment. The resolution of the separation process was found to be directly related to sonication efficiency. By increasing the time of the sonication process, we were able to improve the enrichment of m-SWNTs in the first eluted sample and decrease the s-SWNT contamination. The 1040nm peak in the m-SWNT sample suggested that there were still some s-SWNTs present in this sample and that this process needs to be improved further in order to fully isolate metallic SWNTs. It was unclear what the maximum sonication efficiency that could be achieved was with the gentler sonication process, though this would certainly be the topic of future experiments. Additionally, some of the nanotubes were still bound irreversibly to the gel even after an increased dispersion efficiency. Thus, there were likely some untested factors that had been influencing the passage of the SWNTs

through the gel. Discovering these interactions would also be the subject of future experiments.

References

- Ahadian, S., Ramon-Azcon, J., Estili, M., Liang, X., Ostrovidov, S., Hitoshi, S., . . . Khademhosseini, A. (2014). Hybrid hydrogels containing vertically aligned carbon nanotubes with anisotropic electrical conductivity for muscle myofiber fabrication. *Scientific Reports*, 1-11.
- Barone, V., Hod, O., & Peralta, J. (2012). Modeling of Quasi-One Dimensional Carbon Nanostructures with Density Functional Theory. In J. Leszczynski, *Handbook of Computational Chemistry* (pp. 901-938). Springer Netherlands.
- Clar, J., Batista, C., Youn, S., Bonzong, J., & Ziegler, K. (2013). Interactive Forces between Sodium Dodecyl Sulfate-Suspend Single-Walled Carbon Nanotubes and Agarose Gels. *Journal of the American Chemical Society*, 17758-17767.
- Ghasemi-Mobarakeh, L., Prabhakaran, M., Morshed, M., Nasr-Esfahani, M., & Ramakrishna, S. (2009). Electrical Stimulation of Nerve Cells Using Conductive Nanofibrous Scaffolds for Nerve Tissue Engineering. *Tissue Engineering*, 3605-2619.
- Gheith, M., Pappas, T., Liopo, A., Sinani, V., Shim, B., Motamedi, M., . . . Kotov, N. (2006). Stimulation of Neural Cells by Lateral Currents in Conductive Layer-by-Layer Films of Single-Walled Carbon Nanotubes. *Adv. Mater.*, 2975-2979.
- Kim, J., Kotagiri, N., Kim, J., & Deaton, R. (2006). In Situ fluorescence microscopy visualization and characterization of nanometer-scale carbon nanotubes labeled with 1-pyrenebutanoic acid, succinimidyl ester. *Applied Physics Letters*, 1-3.
- Kotagiri, N., & Kim, J.-W. (2014). Stealth nanotubes: strategies of shielding carbon nanotubes to evade opsonization and improve biodistribution. *International Journal of Nanomedicine*, 85-105.
- Liu, H., Nishide, D., Tanaka, T., & Kataura, H. (2011). Large-scale single-chirality separation of single-wall carbon nanotubes by simple gel chromatography. *Nat. Comm.*, 1-8.

- Liu, X., Gilmore, K., Moulton, S., & Wallace, G. (2009). Electrical stimulation promotes nerve cell differentiation on polypyrrole/poly (2-methoxy-5 aniline sulfonic acid) composites. *J. Neural Eng.*, 1-11.
- MacDonald, R., Laurenzi, B., Viswanathan, G., Ajayan, P., & Stegemann, J. (2005). Collagen-carbon nanotube composite materials as scaffolds in tissue engineering. *Journal of Biomedical Materials Research*, 489-496.
- Niyogi, S., Hamon, M., Hu, H., Zhao, B., Bhowmik, P., Sen, R., . . . Haddon, R. (2002). Chemistry of Single-Walled Carbon Nanotubes. *Acc. Chem. Res.*, 1105-1113.
- Saito, R. (1998). *Physical Properties of Carbon Nanotubes*. Imperial College Press.
- Wilder, J., Venema, L., Rinzler, A., Smalley, R., & Dekker, C. (1998). Electronic Structure of Atomically Resolved Carbon Nanotubes. *Nature*, 59-62.
- Xin, X., Xu, G., & Li, H. (2013). Dispersion and Property Manipulation of Carbon Nanotubes by Self-Assemblies of Amphiphilic Molecules. *Physical and Chemical Properties of Carbon Nanotubes*, 255-273.
- Zhang, H., Wu, B., Hu, W., & Liu, Y. (2011). Separation and/or selective enrichment of single-walled carbon nanotubes based on their electronic properties. *Chem. Soc. Rev.*, 1324-1336.